

# Four-dimensional coherent signalling – constellations and rotations

Magnus Karlsson

Photonics Laboratory, Department of Microtechnology and Nanoscience  
Chalmers University of Technology, Gothenburg, Sweden  
email: magnus.karlsson@chalmers.se

## Paper Summary

*Optical coherent transmission links utilize a four-dimensional (4d) signal space. We review the search for good modulation formats in 4d, as well the properties of these formats under the (subset of all possible) 4d rotations that occur during fiber transmission.*

## Introduction and definitions

Today's coherent optical systems, as pioneered by Sun et al. [1] modulate data on both quadratures on both polarization components, which corresponds to a four-dimensional signal space. The most common scheme of modulation for these systems is to transmit four independent and parallel channels of binary phase-shift keying (BPSK) on the four quadratures, which is often referred to as polarization-multiplexed quadrature PSK, or PM-QPSK. This means that the signaling space is four-dimensional (4d), and any set of signalling levels can be described as a discrete point set in 4d, known as the *constellation*, or *modulation format*.

An optical communication link needs amplifiers to compensate the fiber attenuation, and each optical amplifier adds noise to the signal. After coherent detection the signal plus noise is converted to the electrical domain and sampled to a sequence of discrete symbols with additive white Gaussian noise (AWGN). In the simplest model of a coherent link, the received 4d symbol is thus the transmitted symbol, plus an added 4d noise sample, independent in each quadrature (or coordinate). Thus, given a received 4d symbol, the receiver needs to decide which of the transmitted symbols that is closest to the received one. This is commonly referred to as *maximum likelihood* (ML) detection.

For ML detection the symbol error probability will equal the probability of a received symbol being closer to another symbol than the transmitted one. In the limit of high signal to noise ratio (SNR), this probability depends on the ratio of the noise variance and the minimum distance,  $d_{\min}$ , between any two points in the constellation. For the same, asymptotically high SNR, a constellation will then have an *asymptotic power efficiency*, APE,  $\gamma = d_{\min}^2 / (4E_b)$ , that says how much higher SNR relative to QPSK is needed to have the same SER. Here  $E_b$  is the average energy per bit, and for M constellation points it equals  $E_s / \log_2(M)$ , where  $E_s$  is the symbol energy, geometrically equal to the square distance from the origin, averaged over all M

constellation points. The APE is a strictly geometrical quantity that is useful to compare constellations. It reflects the inherent trade-off in constellation design, which aims for a high  $d_{\min}$  and a low  $E_s$ .

The other important property of a constellation is the *spectral efficiency*, SE, that simply states how many bits per second that is transmitted per unit bandwidth. For a constellation with M points in N-dimensional space this is commonly defined as  $SE = \log_2(M) / (N/2)$ . This defines the SE in units of *bits per symbol per polarization*.

In order to compare the performance of various modulation schemes, one then has to weigh in both the SE and the power efficiency  $\gamma$ . In the following we will perform such a comparison. We will end with a description on how these formats are changed during the transmission in the fiber. The influence of losses and amplification will result in additive noise, but in addition to this the transmission link will perform an unknown and random polarization change, as well as an absolute phase change due to the phase wander between the signal laser and the receiver local oscillator. Both these effects can be described as rotations of the four-dimensional signalling space, and any such rotation need to be undone by the receiver for the signal to be detected without ambiguities. This tutorial will describe, in geometrical terms, the quest for efficient 4d modulation formats as well as the 4d rotations and ambiguities these formats will have.

## Four-dimensional modulation

The most straightforward 4d modulation format is to transmit independent BPSK in each of the four quadratures, or equivalently, independent QPSK in each of the two polarization states. This was the first realized coherent transmission format in modern, DSP-based, coherent detection systems [1], and it transmits 4 bits per 4d symbol, or 2 bits per symbol per polarization. It is referred to as PM-QPSK, has an SE of 2, and  $\gamma = 1$ . In 4d it spans a hypercube, with 16 vertices, given by the set of 4d vectors  $C_1 = \{(\pm 1, \pm 1, \pm 1, \pm 1) / 2\}$ , taken with all sign changes. The question is then whether one can realize a better (more power efficient) format than this. By using sphere packing simulations we showed that, indeed this is possible, for example the constellation  $C_2 = \{(\pm 1, \pm 1, 0, 0), (0, 0, \pm 1, \pm 1)\}$  taken with all sign selections consists of 8 levels and has  $\gamma = 3/2 = 1.76$  dB better sensitivity than PM-QPSK. It can be interpreted as QPSK in *either* of the x or y polarization, and is referred to as polarization-switched QPSK, PS-QPSK [2]. By using sphere packing simulations one can find the best modulation format for every single value of the number

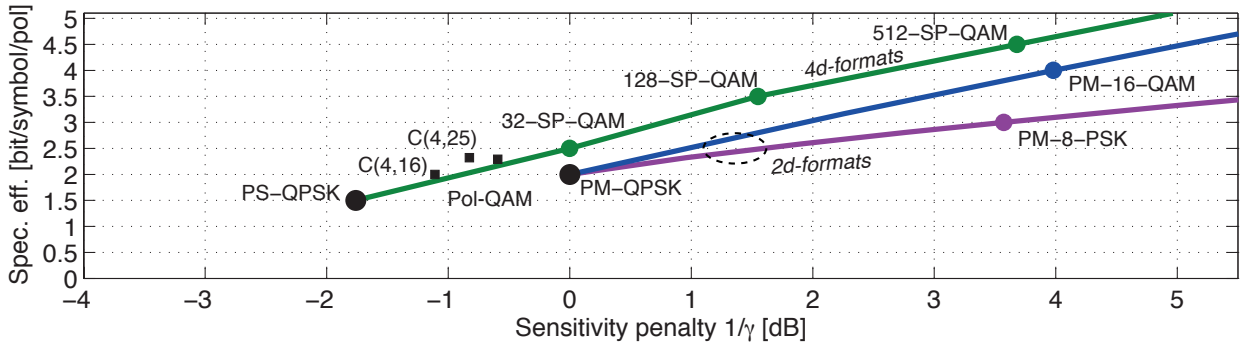


Fig. 1. Spectral efficiency vs sensitivity of some studied 4-dimensional formats. The 2d formats (blue, purple) have less SE and are less power efficient than the 4d formats (green, black).

of levels  $M$ , and that reveals that indeed, PS-QPSK is the most power efficient format of all possible 4d constellations [2,3]. In Fig. 1, the SE vs. sensitivity penalty to formats discussed here is summarized. It was first experimentally realized in [4], and then investigated by many other groups in different contexts [5,6,7]. In [7] an integrated optical modulator, tailored for PS-QPSK, was developed. The simulations also revealed the format  $C(4,16)$ , visualized in Fig. 2, which is the best packing of 16 points in 4d, having a  $\gamma=1.11$  dB [8,9]. Starting from the PM-QPSK format (the 4d hypercube) one can actually add 9 more points without decreasing  $d_{\min}$  or increasing  $E_s$ . The resulting 25-point format,  $C(4,25)$ , is the so-called 24-cell, plus the zero symbol  $(0,0,0,0)$ . The 24 outer points have been realized in the Pol-QAM format [3,10,11], which has around 0.7 dB better asymptotic sensitivity than QPSK.

A nice hierarchy of formats are the *set-partitioning* (SP) formats [12,13], obtainable by removing every second constellation point from regular 4d QAM constellations, or alternatively, by interleaving two QAM formats. For example if PM-16QAM (with  $M=256$ ) is set-partitioned, the SP-128-QAM format arises, or if PM-QPSK is set partitioned one obtains PS-QPSK. If two PM-QPSK constellations are interleaved, the SP-32-QAM format results. All SP-QAM formats have better sensitivity than the regular QAM constellations, which is due to being a subset of the  $D_4$ -lattice, which is a regular structure of points known to produce the best sphere packings in 4d. The SP-128-SP-QAM formats have been analyzed

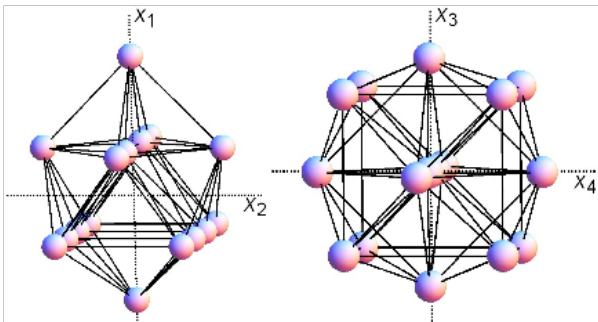


Fig. 2. Two projections of the  $C(4,16)$  constellation. All lines connect nearest neighbours and have unit length.

theoretically in [14] and experimentally in [15-18].

In most cases the novel 4d formats requires slightly different coherent DSP algorithms for polarization and phase tracking, relative to PM-QPSK. Examples of polarization tracking schemes for PS-QPSK are discussed in [6,19]. In general, however the modifications are not significant, and the DSP complexity for the regular 4d formats are comparable to the standard regular QAM formats.

Finally it should be emphasized that many of the proposed 4d formats have simple interpretations in terms of coding. For example, the PS-QPSK and the SP-128-QAM formats can be obtained by a simple parity check code from PM-QPSK and PM-16QAM, respectively [16,20]. In higher than 4 dimensions, formats obtained from well-known forward error correction (FEC) codes. Alternatively, a direct application of an advanced FEC on a non-optimized format may prove as attractive, and this reflects the always-not-so-clear distinction between a modulation format and an FEC code. However there are applications where use of conventional FEC is unwanted, and the use of power-efficient modulation attractive. Links where latency must be limited, or where DSP complexity must be reduced for power saving reasons are examples. Blind channel estimators, or FEC frame detectors where large modulation level separation before the FEC decoder is required, are other examples where these power efficient formats may be valuable.

#### Four-dimensional rotations – an alternative polarization calculus

In order to describe the transmission of coherent 4d signals through the fiber channel a 2d complex Jones vector for signal and a complex  $2 \times 2$  matrix for the transfer matrix is common [21]. In absence of polarization dependent losses, the transfer matrix will be *unitary*, meaning its inverse is its conjugate transpose. The  $2 \times 2$  unitary matrices have 4 degrees of freedom (DOFs), where one models absolute phase changes and 3 models polarization state changes. These usually require different tracking speed in coherent receivers; the phase jitter being on microseconds and polarization drifts on

millisecond time scales. To comply with signal space and detection algorithms, we suggest a reformulation of signal as a real 4d vector of the form of the column vector as  $\mathbf{E} = [\text{Re}(E_x), \text{Im}(E_x), \text{Re}(E_y), \text{Im}(E_y)]^t$ , where  $E_{x,y}$  denotes the signal field polarization components. Fiber transmission can then be expressed with the input-output matrix relation  $\mathbf{E}_{\text{out}} = \mathbf{R} \mathbf{E}_{\text{in}}$ , where  $\mathbf{R}$  denotes a 4x4 real rotation matrix. It turns out that the set of 4x4 real rotations is richer than the set of 2x2 unitary transformations, in that it has 6 DOFs. So what does these extra DOFs correspond to?

In [22], we addressed this question, and showed that 4d rotations can be parameterized into two commuting subgroups, *right-isoclinic* (RI) and *left-isoclinic* (LI), with 3 DOFs each. This is attractive from a polarization calculus point of view, as the 3 RI DOFs can be directly identified with the Poincaré sphere rotation axes. Of the three DOFs for the LI rotations, the first is identified as the absolute phase rotation (which does not affect the polarizations states on the Poincaré sphere), and the remaining two DOFs correspond to *non-physical* rotations, i.e., rotations that cannot occur for propagating photons.

Even if the non-physical rotations cannot arise during transmission, they can be synthesized in DSP, and when applied to the well-known formats like PM-QPSK or PS-QPSK, a very interesting effect arises. While the physical rotations maintain the difference between absolute phase states and polarization states in these constellations, this can be altered by the non-physical rotations. An example with PM-QPSK is shown in Fig. 2. Regular PM-QPSK (constellation  $C_1$ ) is shown with triangles, and can be seen to occupy four polarization states on the Poincaré sphere, and four absolute phase states in the constellation diagrams. One can say that the 16 constellation points of PM-QPSK can be partitioned in four polarization states, each with a four-fold phase degeneracy (or vice versa). Now, after applying a small non-physical rotation, the constellation points marked with circles in Fig 2 arise. We can see that this representation of the hypercube has 8 different polarization states, each with a 2-fold phase degeneracy (which correspond to a sign difference). In other words, the non-physical rotations can alter the polarization-phase content of modulation formats. It allows us to project PM-QPSK as either four polarization states with four phases, or eight polarization states with 2 phases each. This is not possible within the conventional 2x2 Jones matrix formulation. A similar analysis can be done for PS-QPSK; being conventionally seen as 2 polarization states with four phases, a non-physical rotation can transform it into a four-polarization, binary-phase format. This might have practical importance since polarization drifts are usually easier to track than the more rapidly varying phase jitter. Moreover, by being rotations, they do not alter any relevant properties of the formats, such as spectral efficiency or sensitivity.

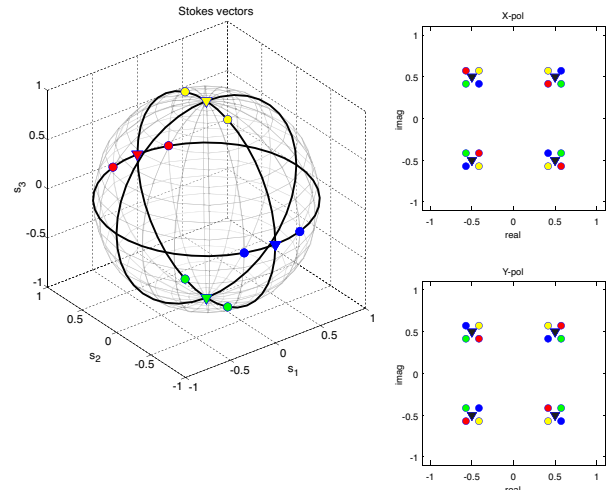


Fig. 3. Stokes vectors and constellations of PM-QPSK (triangles). The circles show the PM-QPSK constellation after a non-physical 4d rotation, with colors referring to the same constellation points. From [22].

However, to utilize this the non-physical rotations for improving coherent receiver performance would require development of new phase- and polarization tracking schemes.

I would like to acknowledge discussions and help from Colin McKinstrie, Erik Agrell, Martin Sjödin, Pontus Johannisson, Tobias Eriksson and other researchers at the Chalmers FORCE center.

## References

1. H. Sun et al., Opt. Exp. 16 (2008) p.873
2. M. Karlsson and E. Agrell Opt. Exp. 17 (2009) p.10814
3. E. Agrell and M. Karlsson, J. Lightwave Technol. 27 (2009) p. 5115
4. M. Sjödin et al., Opt. Exp. 19 (2011), p.7839
5. L. E. Nelson et al., Opt. Exp. 19 (2011), p.10849
6. J. Renaudier et al., J. Lightwave Technol. 30 (2012) p.1312
7. H. Yamazaki et al., OFC (2012), p. PDP5A.8
8. M. Karlsson and E. Agrell, ECOC 2010, p. We.8.C.3
9. J. Karout et al., OFC (2013), p. OW3B.4
10. H. Bülow, OFC (2009), p. OWG.2
11. J. K. Fischer et al., Opt. Exp. 20 (2012), p. B232
12. L. Coelho and N. Hanik, ECOC (2011), p. Mo.2.B.4
13. M. Karlsson and E. Agrell, OFC (2011), p. OTu2C.1
14. M. Sjödin et al., Opt. Exp. 20 (2012), p. 8356
15. T. Eriksson et al., OFC (2013), p. OTu2C.1
16. H. Zhang et al., OFC (2013), p. PDP5A.6
17. J. Renaudier et al., OFC (2013), p. OTu3B.1
18. R. van Uden et al., OFC (2014), p. W4J.4
19. P. Johannisson et al., Opt. Exp. 19 (2011) p.7734
20. B. Krongold et al., IEEE Photon. Technol. Lett. 24, (2012) p.203
21. S. Betti et al., J. Lightwave Technol. 9 (1991) p. 514
22. M. Karlsson, J. Lightwave Technol. 32 (2014) p.1246